

# Naturalness, Weak Scale Supersymmetry and the Prospect for the Observation of Supersymmetry at the Tevatron and at the LHC

Kwok Lung Chan, Utpal Chattopadhyay and Pran Nath  
 Department of Physics, Northeastern University  
 Boston, MA 02115-5005

## Abstract

Naturalness bounds on weak scale supersymmetry in the context of radiative breaking of the electro-weak symmetry are analyzed. In the case of minimal supergravity it is found that for low  $\tan\beta$  and for low values of fine tuning  $\Phi$ , where  $\Phi$  is defined essentially by the ratio  $\mu^2/M_Z^2$  where  $\mu$  is the Higgs mixing parameter and  $M_Z$  is the Z boson mass, the allowed values of the universal scalar parameter  $m_0$ , and the universal gaugino mass  $m_{1/2}$  lie on the surface of an ellipsoid with radii fixed by  $\Phi$  leading to tightly constrained upper bounds  $\sim \sqrt{\Phi}$ . Thus for  $\tan\beta \leq 2(\leq 5)$  it is found that the upper limits for the entire set of sparticle masses lie in the range  $< 700$  GeV ( $< 1.5$ TeV) for any reasonable range of fine tuning ( $\Phi \leq 20$ ). However, it is found that there exist regions of the parameter space where the fine tuning does not tightly constrain  $m_0$  and  $m_{1/2}$ . Effects of non-universalities in the Higgs sector and in the third generation sector on naturalness bounds are also analyzed and it is found that non-universalities can significantly affect the upper bounds. It is also found that achieving the maximum Higgs mass allowed in supergravity unified models requires a high degree of fine tuning. Thus a heavy sparticle spectrum is indicated if the Higgs mass exceeds 120 GeV. The prospect for the discovery of supersymmetry at the Tevatron and at the LHC in view of these results is discussed.

## 1 Introduction

One of the important elements in supersymmetric model building is the issue of the mass scale of the supersymmetric particles. There is the general expectation that this scale should be of the order of the scale of the electro-weak physics, i.e., in the range of a TeV. This idea is given a more concrete meaning in the context of supergravity unification[1] where one has spontaneous breaking of the electro-weak symmetry by radiative corrections[2]. Radiative breaking of the electro-weak symmetry relates the scale of supersymmetry soft breaking terms directly to the Z boson mass. This relationship then tells us that the soft SUSY breaking scale should not be much larger

than the scale of the Z boson mass otherwise a significant fine tuning will be needed to recover the Z boson mass. The above general connection would be thwarted if there were large internal cancellations occurring naturally within the radiative breaking condition which would allow  $m_0$  and  $m_{1/2}$  disproportionately large for a fixed fine tuning. We shall show that precisely such a situation does arise in certain domains of the supergravity parameter space.

The simplest fine tuning criterion is to impose the constraint that  $m_0, m_{\tilde{g}} < 1$  TeV where  $m_0$  is the universal soft SUSY breaking scalar mass in minimal supergravity and  $m_{\tilde{g}}$  is the gluino mass. The above criterion is easy to implement and has been used widely in the literature (for a review see Ref.[3]). A more involved fine tuning criterion is given in Ref.[4]. However, it appears that the criterion of Ref.[4] is actually a measure of the sensitivity rather than of fine tuning[5, 6]. Another naturalness criterion is proposed in Ref.[6] and involves a distribution function. Although the distribution function is arbitrary the authors show that different choices of the function lead numerically to similar fine tuning limits.

In the analysis of this paper we use the fine tuning criterion introduced in Ref.[7] in terms of the Higgs mixing parameter  $\mu$  which has several attractive features. It is physically well motivated, free of ambiguities and easy to implement. Next we use the criterion to analyze the upper limits of sparticle masses for low values of  $\tan\beta$ , i.e.,  $\tan\beta \leq 5$ . In this case one finds that  $m_0$  and  $m_{1/2}$  allowed by radiative breaking lie on the surface of an ellipsoid, and hence the upper limits of the sparticle masses are directly controlled by the radii of the ellipsoid which in turn are determined by the choice of fine tuning. For instance, one finds that if one is in the low  $\tan\beta$  end of  $b - \tau$  unification[8] with the top mass in the experimental range, i.e.  $\tan\beta \approx 2$ , then for any reasonable range of fine tuning the sparticle mass upper limits for the entire set of SUSY particles lie within the mass range below 1 TeV. Further, one finds that the light Higgs mass lies below 90 GeV under the same constraints. Thus in this case discovery of supersymmetry at the LHC is guaranteed according to any reasonable fine tuning criterion. Next the paper explores larger values of  $\tan\beta$ , i.e.,  $\tan\beta \geq 10$  and here one finds that  $m_0$  and  $m_{1/2}$  for moderate values of fine tuning do not lie on the surface of an ellipsoid; rather one finds that they lie on the surface of a hyperboloid. In this case  $m_0$  and  $m_{1/2}$  are not bounded by the  $\mu$  constraint equation and large values of  $m_0$  and  $m_{1/2}$  can result with a fixed fine tuning.

Effect of non-universalities on naturalness is also analyzed. Again one finds phenomena similar to the ones discussed above, although the domains in which these phenomena occur are shifted relative to those in the universal case. One of the important results that emerges is that the upper limits of sparticle masses can be dramatically affected by non-universalities. These results have important implications for the discovery of supersymmetry at the Tevatron and the LHC.

Our analysis is carried out in the framework of supergravity models with gravity mediated breaking of supersymmetry[9, 1, 3]. This class of models possesses many attractive features. One of the more attractive features of these models is that with R parity invariance the lightest neutralino is also the lightest supersymmetric particle over most of the parameter space of the theory and hence a candidate for cold dark matter. Precision renormalization group analyses show[10] that these models can accommodate

just the right amount of dark matter consistent with the current astrophysical data[11, 12]. However, in this work we shall not impose the constraint of dark matter.

The outline of the paper is as follows: In Sec.2 we give a brief discussion of the fine tuning measure used in the analysis. In Sec.3 we use this criterion to discuss the upper limits on the sparticle masses in minimal supergravity for low  $\tan\beta$ , i.e.,  $\tan\beta \leq 5$  and show that the allowed solutions to radiative breaking lie on the surface of an ellipsoid. In Sec.4 we discuss naturalness in beyond the low  $\tan\beta$  region. Here we show that radiative breaking of the electro-weak symmetry leads to the soft SUSY breaking parameters lying on the surface of a hyperboloid. In Sec.5 we discuss the effects of non-universalities on the upper limits. In Sec.6 we show that a high degree of fine tuning is needed to have the light Higgs mass approach its maximum upper limit. The limits on  $\Phi$  from the current data are discussed in sec.7. Implications of these results for the discovery of supersymmetric particles at colliders is also discussed in Secs. 3-6. Conclusions are given in Sec.8.

## 2 Measure of Naturalness

We give below an improved version of the analysis of the fine tuning criterion given in Ref.[7]. The radiative electro-weak symmetry breaking condition is given by

$$\frac{1}{2}M_Z^2 = \lambda^2 - \mu^2 \quad (1)$$

where  $\lambda^2$  is defined by

$$\lambda^2 = \frac{\bar{m}_{H_1}^2 - \bar{m}_{H_2}^2 \tan^2 \beta}{\tan^2 \beta - 1} \quad (2)$$

Here  $\bar{m}_{H_i}^2 = m_{H_i}^2 + \Sigma_i$  (i=1,2) where  $\Sigma_i$  arise from the one loop corrections to the effective potential[13]. The issue of fine tuning now revolves around the fact that a cancellation is needed between the  $\lambda^2$  term and the  $\mu^2$  term to arrange the correct experimental value of  $M_Z$ . Thus a large value of  $\lambda^2$  would require a large cancellation from the  $\mu^2$  term resulting in a large fine tuning. This idea can be quantified by defining the fine tuning parameter  $\Phi$  so that

$$\Phi^{-1} = 4 \frac{\lambda^2 - \mu^2}{\lambda^2 + \mu^2} \quad (3)$$

(The factor of 4 on the right hand side in Eq.(3) is just a convenient normalization.) The expression for  $\Phi$  can be simplified by inserting in the radiative breaking condition Eq.(1). We then get

$$\Phi = \frac{1}{4} + \frac{\mu^2}{M_Z^2} \quad (4)$$

The result above is valid with the inclusion of both the tree and the loop corrections to the effective potential. ( $\Phi$  is related to the fine tuning parameter  $\delta$  defined in Ref.[7] by  $\Phi = \delta^{-1}$ ). For large  $\mu$  one has  $\Phi \sim \frac{\mu^2}{M_Z^2}$ , a result which has a very direct intuitive meaning. A large  $\mu$  implies a large cancellation between the  $\lambda^2$  term and the  $\mu^2$  term

in Eq.1 to recover the Z boson mass and thus leads to a large fine tuning. Typically a large  $\mu$  implies large values for the soft supersymmetry breaking parameters  $m_0$  and  $m_{1/2}$  and thus large values for the sparticle masses. However, large cancellation can be enforced by the internal dynamics of radiative breaking itself. In this case a small  $\mu$  and hence a small fine tuning allows for relatively large values of  $m_0$  and of  $m_{1/2}$ . We show that precisely such a situation arises for certain regions of the parameter space of both the minimal model as well as for models with non-universalities.

### 3 Upper Bounds on Sparticle Masses in Minimal Supergravity

We discuss now the upper bounds on the sparticle masses that arise under the criterion of fine tuning we have discussed above. Using the radiative electro-weak symmetry breaking constraint and ignoring the b-quark couplings, justified for small  $\tan\beta$ , we may express the fine tuning parameter  $\Phi_0$  in the form

$$\Phi_0 = -\frac{1}{4} + \left(\frac{m_0}{M_Z}\right)^2 C_1 + \left(\frac{A_0}{M_Z}\right)^2 C_2 + \left(\frac{m_{1/2}}{M_Z}\right)^2 C_3 + \left(\frac{m_{1/2} A_0}{M_Z^2}\right) C_4 + \frac{\Delta\mu_{loop}^2}{M_Z^2} \quad (5)$$

where

$$C_1 = \frac{1}{t^2 - 1} \left(1 - \frac{3D_0 - 1}{2} t^2\right), C_2 = \frac{t^2}{t^2 - 1} k \quad (6)$$

$$C_3 = \frac{1}{t^2 - 1} (g - t^2 e), C_4 = -\frac{t^2}{t^2 - 1} f, \Delta\mu_{loop}^2 = \frac{\Sigma_1 - t^2 \Sigma_2}{t^2 - 1} \quad (7)$$

Here  $t \equiv \tan\beta$ , e, f, g, k and the sign conventions of  $A_0$  and  $\mu$  are as defined in Ref.[14],  $D_0$  is defined by

$$D_0 = 1 - (m_t/m_f)^2, \quad m_f \simeq 200 \sin\beta \text{ GeV} \quad (8)$$

and  $\Sigma_1$  and  $\Sigma_2$  are as defined in Ref. [13].

To investigate the upper limits on  $m_0$  and  $m_{1/2}$  consistent with a given fine tuning it is instructive to write Eq.(5) in the form

$$C_1 m_0^2 + C_3 m_{1/2}^2 + C_2' A_0^2 + \Delta\mu_{loop}^2 = M_Z^2 \left(\Phi_0 + \frac{1}{4}\right) \quad (9)$$

where

$$m_{1/2}' = m_{1/2} + \frac{1}{2} A_0 \frac{C_4}{C_3}, \quad C_2' = C_2 - \frac{1}{4} \frac{C_4^2}{C_3} \quad (10)$$

and  $\Delta\mu_{loop}^2$  is the loop correction. Now for the universal case one finds that the loop corrections to  $\mu$  are generally small for  $\tan\beta \leq 5$  in the region of fine tuning of  $\Phi_0 \leq 20$ . Further, using renormalization group analysis one finds that  $C_2' > 0$  and  $C_3 > 0$  and at least for the range of fine tuning  $\Phi_0 \leq 20$ ,  $C_1 > 0$  (see Table 1). Thus in this case defining

$$a^2 = M_Z^2 \frac{\Phi + \frac{1}{4}}{C_3}, b^2 = M_Z^2 \frac{\Phi + \frac{1}{4}}{C_1}, \quad c^2 = M_Z^2 \frac{\Phi + \frac{1}{4}}{C_2'} \quad (11)$$

we find that for  $\tan\beta \leq 5$ ,  $\Phi_0 \leq 20$  the radiative breaking condition can be approximated by

$$\frac{m_{1/2}^2}{a^2} + \frac{m_0^2}{b^2} + \frac{A_0^2}{c^2} \simeq 1 \quad (12)$$

and the renormalization group analysis shows that at the scale  $Q = M_Z$  the quantities  $a^2$ ,  $b^2$  and  $c^2$  are positive. Fixing the fine tuning parameter  $\Phi_0$  fixes  $a, b$ , and  $c$  and one finds that  $m_0$  and  $m_{1/2}$  are bounded as they lie on the boundary of an ellipse. Further Eq.(12) implies that the upper bounds on  $m_0$  and  $m_{1/2}$  increase as  $\sim \sqrt{\Phi_0}$  for large  $\Phi_0$ . A similar dependence on fine tuning was observed in the analysis of ref. 4.

We give now the full analysis without the approximation of Eq.(12). We consider the case of  $\tan\beta = 2$  first which lies close to the low end of the  $\tan\beta$  region of  $b$ - $\tau$  unification with the top mass taken to lie in the experimental range[8]. In Fig.1a. we give the contour plot of the upper limits for the parameters  $m_0$  and  $m_{1/2}$  in the  $m_0 - m_{1/2}$  plane for the case of  $\tan\beta = 2$  and  $m_t = 175$  GeV for  $2.5 \leq \Phi_0 \leq 20$ . As expected, one finds that the contours corresponding to larger values of  $m_0$  and  $m_{1/2}$  require larger values of  $\Phi_0$ . The upper limits of the mass spectra for the same set of parameters as in Fig.1a are analyzed in Fig.1b - Fig.1d. In Fig.1b the upper limits of the mass spectra of the heavy Higgs, the first two generation squarks, and the gluino are given. We find that the mass of the squark and of the gluino are very similar over essentially the entire range of  $\Phi_0$ . Upper limits of  $\tilde{e}$ ,  $\tilde{t}_1$ ,  $\tilde{t}_2$  are given in Fig.1c. In Fig.1d we exhibit the upper limits for the light Higgs, the chargino, and the lightest neutralino. We note that except for small values of  $\Phi_0$  one finds that the scaling laws [15](e.g.  $m_{\chi_1^0} \simeq \frac{1}{2}m_{\chi_1^\pm}$ ) are obeyed with a high degree of accuracy. We note that the Higgs mass upper limit in this case falls below 85-90 GeV for  $\Phi_0 \leq 20$ . At the Tevatron in the Main Injector era one will be able to detect charginos using the trileptonic signal[16] with masses up to 230 GeV with  $10\text{fb}^{-1}$  of integrated luminosity[17, 18]. Reference to Fig.1d shows that the above implies that the upper limit of chargino masses for the full range of  $\Phi_0 \leq 20$  will be accessible at the Tevatron.

For the gluino the mass range up to 450 GeV will be accessible at the Tevatron in the Main Injector era with  $25\text{fb}^{-1}$  of integrated luminosity. This means that one can explore gluino mass limits up to  $\Phi_0=10$  for  $\tan\beta = 2$ . However, at the LHC gluino masses in the range 1.6-2.3 TeV [19]/1.4-2.6 TeV[20] for most values of  $\mu$  and  $\tan\beta$  will be accessible and recent analyses show that the accuracy of the  $m_{\tilde{g}}$  mass measurement can be quite good, i.e., to within 1-10% depending on what part of the supergravity parameter space one is in[21]. Thus for  $\tan\beta = 2$  one will be able to observe and measure with reasonable accuracy the masses of the charginos, the gluino, and the squarks for the full range of values of  $\Phi_0 \leq 20$  at the LHC. It has recently been argued that the NLC, where even more accurate mass measurements[22, 23, 24] are possible, will allow one to use this device for the exploration of physics at the post-GUT and string scales[25]. The NLC also offers the possibility of testing a good part of the parameter space for the  $\tan\beta = 2$  model. The analysis given in Table 2 shows that the full sparticle mass spectrum for  $\tan\beta=2$  can be tested at the NLC with  $\sqrt{s} = 1$  TeV for  $\Phi_0 \leq 10$  and over the entire range  $\Phi_0 \leq 20$  with  $\sqrt{s} = 1.5$  TeV.

We discuss next the upper limit of sparticle masses for  $\tan\beta = 5$ . In Fig.2a we give the contour plot of  $m_0$  and  $m_{1/2}$  upper limits in the  $m_0 - m_{1/2}$  plane for the same value

of the top mass and in the same  $\Phi_0$  range as in Fig.1a. Here we find that for fixed  $\Phi_0$  the contours are significantly further outwards compared to the case for  $\tan\beta = 2$ . Correspondingly the upper limits of the mass spectra for the same value of  $\Phi_0$  are significantly larger in Fig. 2b-2d relative to those given in Figs. 1b-1d. In this case the light chargino mass lies below 243 GeV for  $\Phi_0 \leq 20$  and thus the upper limits for values of  $\Phi_0 \leq 20$  could be probed at the Tevatron in the Main Injector era where chargino masses up to 280 GeV will be accessible with  $100\text{fb}^{-1}$  of integrated luminosity[17, 18]. Similarly in this case the gluino mass lies below 873 GeV for  $\Phi_0 \leq 20$  and thus the upper limit for values of  $\Phi_0 \leq 20$  could be probed at the LHC which as mentioned above can probe gluino masses in the mass range of 1.6–2.3 TeV[19]/ 1.4–2.6 TeV[20]. LHC can probe squark masses up to 2-2.5 TeV, so squark masses of the above size should be accessible at the LHC. A full summary of the results for values of  $\tan\beta=2-20$  is given in Table 2 where the sparticle mass limits in the range  $2.5 \leq \Phi_0 \leq 20$  are given. The analysis tells us that for a reasonable constraint on  $\Phi_0$ , i.e.  $\Phi_0 \leq 20$ , the gluino and the squarks must be discovered at the LHC for the values of  $\tan\beta \leq 5$ .

## 4 Regions Of the Hyperbolic Constraint

In this section we discuss the possibility that in certain regions of the supergravity parameter space the sparticle spectrum can get large even for modest values of the fine tuning parameter  $\Phi_0$ . This generally happens in regions where the loop corrections to  $\mu$  are large. For example, in contrast to the case of small  $\tan\beta$  one finds that for the case of large  $\tan\beta$  the loop corrections to  $\mu$  can become rather significant. In this case the size of the loop corrections to  $\mu$  depends sharply on the scale  $Q_0$  where the minimization of the effective potential is carried out. In fact, in this case there is generally a strong dependence on  $Q_0$  of both the tree and the loop contributions to  $\mu$  which, however, largely cancel in the sum, leaving the total  $\mu$  with a sharply reduced but still non-negligible residual  $Q_0$  dependence. An illustration of this phenomenon is given in Fig.3. The choice of  $Q_0$  where one carries out the minimization of the effective potential is of importance because we can choose a value of  $Q_0$  where the loop corrections are small so that we can carry out an analytic analysis similar to the one in Sec.3. (For example, for the case of Fig. 3 the loop correction to  $\mu$  is minimized at  $Q_0 \approx 1$  TeV). Generally we find the value  $Q_0$  at which the loop correction to  $\mu$  is minimized to be about the average of the smallest and the largest sparticle masses, a value not too distant from  $\sqrt{m_{\tilde{t}_L} m_{\tilde{t}_R}}$ , which is typically chosen to minimize the 2-loop correction to the Higgs mass[26, 12]. Choosing a value  $Q_0$  where the loop correction is small ( $Q_0$  is typically greater than 1 TeV here), and following the same procedure as in Sec.3 we find that this time  $\text{sign}(C_1(Q_0))=-1$  (see entries for the case  $\tan\beta = 10, 20$  in Table 1 and see also fig. 5a). There are now two distinct possibilities: case A and case B which we discuss below.

**Case A:** This case corresponds to

$$(\Phi_0 + \frac{1}{4})M_Z^2 - C'_2 A_0^2 > 0 \quad (13)$$

and occurs for relatively small values of  $|A_0|$ . Here the radiative breaking equation takes the form

$$\frac{m_{1/2}^2}{\alpha^2(Q_0)} - \frac{m_0^2}{\beta^2(Q_0)} \simeq 1 \quad (14)$$

where

$$\alpha^2 = \frac{|(\Phi_0 + \frac{1}{4})M_Z^2 - C'_2 A_0^2|}{|C_3|} \quad (15)$$

and

$$\beta^2 = \frac{|(\Phi_0 + \frac{1}{4})M_Z^2 - C'_2 A_0^2|}{|C_1|} \quad (16)$$

The appearance of a minus sign changes intrinsically the character of the constraint of the electro-weak symmetry breaking. One finds now that unlike the previous case, where  $m_0$  and  $m_{1/2}$  lie on the boundary of an ellipse for fixed  $A_0$  (see Fig.4a and also Figs.1a and 2a), here they lie on a hyperbola. A diagrammatic representation of the constraint of Eq.(14) is given in Fig.4b-4c. The position of the apex of the hyperbola depends on  $A_0$  as can be seen from Fig.4c. The choice of  $\Phi$  itself does not put an upper bound on  $m_0$  and  $m_{1/2}$  and consequently they can get large for a fixed fine tuning unless other constraints intervene. Thus in this case the rule that the upper bounds are proportional to  $\sqrt{\Phi_0}$  breaks down. In fact from Eq.(14)-(16) we see that for large  $m_0$  and  $m_{1/2}$  one has

$$m_0 \simeq \sqrt{\frac{|C_3|}{|C_1|}} m'_{1/2} \quad (17)$$

and thus independent of  $\Phi_0$ . Thus the hyperbolae for different values of fine tuning have the same asymptote independent of  $\Phi_0$  as illustrated in Fig.4b.

**Case B:** This case corresponds to

$$(\Phi_0 + \frac{1}{4})M_Z^2 - C'_2 A_0^2 < 0 \quad (18)$$

and occurs for relatively large values of  $A_0$ . Here the radiative breaking equation takes the form

$$\frac{m_0^2}{\beta^2(Q_0)} - \frac{m_{1/2}^2}{\alpha^2(Q_0)} \simeq 1 \quad (19)$$

A diagrammatic representation of this case is given in Fig 4d. As in Case A, here also  $m_0$  and  $m_{1/2}$  lie on a hyperbola, with the position of the apex determined by the value of  $A_0$ . Again here as in case A the choice of  $\Phi_0$  itself does not control the upper bound on  $m_0$  and  $m_{1/2}$ . This can be seen from Fig.4d where the hyperbolae for different values of the fine tuning have the same asymptote independent of  $\Phi_0$  just as in case A. We emphasize that the analytic analysis based on Eqs.(14) and (19) is for illustrative purposes only, and the results presented in this paper are obtained including the b-quark couplings and including the full one loop corrections to  $\mu$ . In Fig.5b we present a numerical analysis of the allowed region of  $m_0$  and  $m_{1/2}$ . One finds that the cases  $A_0 = 0$  and  $A_0 = 500$  GeV show that  $m_0$  and  $m_{1/2}$  lie on a branch of a hyperbola

and simulate the illustration of Fig.4c. This is what one expects for the small  $A_0$  case. Similarly for the cases  $A_0 = -1000$  GeV and  $A_0 = -2000$  GeV in Fig.5b,  $m_0$  and  $m_{1/2}$  lie on a branch of a hyperbola and simulate the illustration of the right hyperbola in Fig.4d as is appropriate for a large negative  $A_0$ . Similarly for the case  $A_0 = 1000$  GeV in Fig.5b,  $m_0$  and  $m_{1/2}$  again lie on a branch of a hyperbola and simulate the illustration of the left hyperbola in Fig.4d. A similar analysis for  $\tan\beta = 20$  can be found in Fig.5c. Thus one finds that the results of the analytic analysis are supported by the full numerical analysis.

## 5 Effects of Non-universal Soft SUSY Breaking

The analysis of Secs. 3 and 4 above is carried out under the assumption of universal soft supersymmetry boundary conditions at the GUT scale. These universal boundary conditions arise from the assumption of a flat Kahler potential. However, the framework of supergravity unification[1, 3] allows for more general Kahler structures and hence for non-universalities in the soft supersymmetry breaking parameters[27, 25]. In the analysis of this section we shall assume universalities in the soft supersymmetry breaking parameters in the first two generations of matter but allow for non-universalities in the Higgs sector[25, 28, 29, 30] and in the third generation of matter[25, 30, 31]. It is convenient to parametrize the non-universalities in the following fashion. In the Higgs sector one has

$$m_{H_1}^2 = m_0^2(1 + \delta_1), \quad m_{H_2}^2 = m_0^2(1 + \delta_2) \quad (20)$$

Similarly in the third generation sector one has

$$m_{\tilde{Q}_L}^2 = m_0^2(1 + \delta_3), \quad m_{\tilde{U}_R}^2 = m_0^2(1 + \delta_4) \quad (21)$$

A reasonable range for the non-universality parameters is  $|\delta_i| \leq 1$  (i=1-4). Inclusion of non-universalities modifies the electro-weak symmetry breaking equation determining the parameter  $\mu^2$ , and leads to corrections to the fine tuning parameter  $\Phi$ . One finds that with these non-universality corrections  $\Phi$  is given by

$$\Phi = -\frac{1}{4} + \left(\frac{m_0}{M_Z}\right)^2 C'_1 + \left(\frac{A_0}{M_Z}\right)^2 C_2 + \left(\frac{m_{\frac{1}{2}}}{M_Z}\right)^2 C_3 + \left(\frac{m_{\frac{1}{2}} A_0}{M_Z^2}\right) C_4 + \frac{\Delta\mu_{loop}^2}{M_Z^2} \quad (22)$$

where

$$C'_1 = \frac{1}{t^2 - 1} \left(1 - \frac{3D_0 - 1}{2} t^2\right) + \frac{1}{t^2 - 1} (\delta_1 - \delta_2 t^2 - \frac{D_0 - 1}{2} (\delta_2 + \delta_3 + \delta_4) t^2) + \frac{3t^2 + 1}{5t^2 - 1} \frac{pS_0}{m_0^2} \quad (23)$$

and  $C_2$ ,  $C_3$  and  $C_4$  are as defined in Eqs.(6) and (7). Here  $S_0$  is the trace anomaly term

$$S_0 = Tr(Ym^2) \quad (24)$$



evaluated at the GUT scale  $M_G$ . It vanishes in the universal case since  $\text{Tr}(Y)=0$ , but contributes when non-universalities are present.  $p$  is as defined in Ref. [30]. Numerically for  $M_G = 10^{16.2}$  GeV and  $\alpha_G = 1/24$  one has  $p \simeq 0.045$ . Eq.(23) shows how important the effects of non-universalities are on  $\Phi$ . For a moderate value of  $m_0 = 250$  GeV the factor  $(m_0/M_Z)^2$  is  $\sim 7.5$  and since  $\delta_i \sim O(1)$ ,  $\Phi$  gets a huge shift. This means that the upper limits of the sparticle masses are going to be sensitively dependent on the magnitudes and signatures of  $\delta_i$ .

It is instructive to write the radiative breaking equation Eq.(21) with non-universalities in a form similar to Eq.(9). We get

$$C'_1 m_0^2 + C_3 m_{1/2}^2 + C'_2 A_0^2 + \Delta\mu_{loop}^2 = M_Z^2(\Phi + \frac{1}{4}) \quad (25)$$

where  $C'_1$  is defined in Eq.(23), and  $C_2$  and  $C_3$  are defined in Eq.(7) and where  $\Delta\mu_{loop}^2$  is the loop correction. We discuss the case of non-universalities in the Higgs sector first and consider two extreme examples within the constraint of  $|\delta_i| \leq 1$  (i=1-2). These are (i)  $\delta_1 = 1$ ,  $\delta_2 = -1$ , and (ii)  $\delta_1 = -1$ ,  $\delta_2 = 1$ , with  $\delta_3 = 0 = \delta_4$  in both cases. For case(i) we find from Eq.(23) that the non-universalities make a positive contribution to  $C'_1$ , and thus  $C'_1 > 0$  (see Table 3). As for the universal case the loop corrections in this case are generally small. Thus in this case one finds that the radiative breaking condition takes the form

$$\frac{m_{1/2}^2}{a^2} + \frac{m_0^2}{b'^2} + \frac{A_0^2}{c^2} \simeq 1 \quad (26)$$

where  $a$  and  $c$  are defined by Eq.(11) and  $b'$  is defined by

$$b'^2 = M_Z^2 \frac{(\Phi + \frac{1}{4})}{|C'_1|}, \quad (27)$$

As in the universal case (see Figs.1a, 2a and 4a) here also for given fine tuning one finds that  $m_0$  and  $m_{1/2}$  are bounded as they lie on the boundary of an ellipse. Further,  $C'_1 > C_1$  implies that a given  $\Phi$  corresponds effectively to a smaller  $\Phi_0$ , and hence admits smaller values of the upper limits of the squark masses relative to the universal case. This is what is seen in Table 4. Here we find that the upper limits are generally decreased over the full range of  $\Phi$ .

For case(ii) the situation is drastically different. Here the non-universalities make a negative contribution driving  $C'_1$  negative (see Table 3) and further  $C'_1$  remains negative in the relevant  $Q$  range (see Table 5). Thus the radiative breaking solutions no longer lie on the boundary of an ellipse. The analysis in this case is somewhat more complicated in that the loop corrections to  $\mu^2$  at the scale  $Q = M_Z$  are large. For illustrative purposes one may carry out an analysis similar to the one discussed in Sec.3 and go to the scale  $Q=Q'_0$ , where the loop corrections to  $\mu^2$  are negligible. Again there are two cases and we discuss these below.

**Case C:** This case is defined by Eq.(13) and the radiative symmetry breaking constraint here reads

$$\frac{m_{1/2}^2}{\alpha^2(Q'_0)} - \frac{m_0^2}{\beta'^2(Q'_0)} \simeq 1 \quad (28)$$

where

$$\beta'^2 = \frac{|(\Phi + \frac{1}{4})M_Z^2 - C'_2 A_0^2|}{|C'_1|} \quad (29)$$

Eq.(28) shows that the radiative symmetry breaking constraint in this case is a hyperbolic constraint.

**Case D:** This case is defined by Eq.(18) and the radiative symmetry breaking constraint here reads

$$\frac{m_0^2}{\beta'^2(Q'_0)} - \frac{m_{1/2}^2}{\alpha^2(Q'_0)} \simeq 1 \quad (30)$$

Again the radiative symmetry breaking constraint is a hyperbolic constraint.

Cases C and D are similar to the cases A and B except that here  $m_0$  and  $m_{1/2}$  lie on a hyperbola even for small  $\tan\beta$  because of the effect of the specific nature of the non-universalities in this case. Thus here it is the non-universalities which transform the radiative breaking equation from an ellipse to a hyperbola. Of course  $m_0$  and  $m_{1/2}$  do not become arbitrarily large, since eventually other constraints set in and limit the allowed values of  $m_0$  and  $m_{1/2}$ . Results of the analysis are given in Fig.(6). One finds that  $m_0$  and  $m_{1/2}$  indeed can become large for a fixed fine tuning.

To understand the effects of the non-universalities in the third generation in comparison to the non-universalities in the Higgs sector it is useful to express  $\Delta\Phi$  in the following alternate form

$$\Delta\Phi = \frac{1}{t^2 - 1}(\delta_1 - (1 - \frac{1}{2}(\frac{m_t}{m_f})^2)\delta_2 t^2 + \frac{1}{2}(\frac{m_t}{m_f})^2(\delta_3 + \delta_4)t^2)(\frac{m_0}{M_Z})^2 + \frac{3}{5} \frac{t^2 + 1}{t^2 - 1} \frac{pS_0}{M_Z^2} \quad (31)$$

Since  $m_t < m_f$  one has  $(1 - \frac{1}{2}(\frac{m_t}{m_f})^2) > 0$  which implies that the effect of a negative(positive)  $\delta_2$  can be simulated by a positive(negative) value of  $\delta_3$  or by a positive(negative) value of  $\delta_4$ . This correlation can be seen to hold by a comparison of Tables 4 and 6. As in the case of Table 4 where a positive  $\delta_1$  and a negative  $\delta_2$  leads to lowering of the upper limits on squark masses, we find that a positive  $\delta_3$  or a positive  $\delta_4$  produces a similar effect. The analysis of Table 6 where we choose  $(\delta_1, \delta_2, \delta_3, \delta_4) = (0, 0, 1, 0)$  supports this observation. A similar correlation can be made between the case of  $\delta_1 < 0, \delta_2 > 0$  and the case  $\delta_3 + \delta_4 < 0$  by the comparison given above. We note, however, that the effects of non-universalities in the Higgs sector and in the third generation sector are not identical in every respect as they enter in different ways in other parts of the spectrum. However, the gross features of the upper limits of squarks in Table 6 can be understood by the rough comparison given above.

A comparison of Tables 2, 4, and 6 shows that the non-universalities have a remarkable effect on the upper limits of sparticle masses. One finds that the upper limits on the sparticle masses can increase or decrease dramatically depending on the type of non-universality included in the analysis. The prospects for the observation of sparticles at colliders are thus significantly affected. For the case of Table 4 and 6 one finds that the sparticle spectrum falls below 1 TeV in the range  $\tan\beta \leq 5, \Phi \leq 20$ . Thus in this case the gluino and the squarks should be discovered at the LHC and all of the other sparticles should also be discovered over most of the mass ranges in Table 4.

In contrast for the case of non-universality of Table.6 we find that the nature of non-universal contribution is such that squark masses can exceed the discovery potential of even the LHC. The analysis given above is for  $\mu < 0$ . A similar analysis holds with essentially the same general conclusions for the  $\mu > 0$  case.

## 6 Upper Limit on the Higgs Mass

One of the most interesting part of our analysis concerns the dependence of the Higgs mass upper limits on  $\Phi_0$ . For the analysis of the Higgs mass upper limits we have taken account of the one loop corrections to the masses and further chosen the scale  $Q$  which minimizes the two loop corrections[26, 12]. For  $\tan\beta = 2$  the upper limit on the Higgs mass increases from 60 GeV at  $\Phi_0=2.5$  GeV to 86 GeV at  $\Phi_0=20$ . Further from the successive entries in this case in Table 2 we observe that in each of the cases where an increment in the Higgs mass occurs, one requires a significant increase in the value of  $\Phi_0$ . The same general pattern is repeated for larger values of  $\tan\beta$ . Thus for  $\tan\beta = 5$  the Higgs mass increases from 97 GeV to 116 GeV as  $\Phi_0$  increases from 2.5 to 20. In Fig.7 we exhibit the upper bound on the Higgs mass as a function of  $\tan\beta$ . From the analysis of Table 2 and Fig.7 one can draw the general conclusion that the Higgs mass upper limit is a sensitive function of  $\tan\beta$  and  $\Phi_0$ . For values of  $\tan\beta$  near the low end, i.e.  $\tan\beta \approx 2$ , the upper limit of the Higgs mass lies below 85-90 GeV for any reasonable range of fine tuning, i.e.  $\Phi_0 \leq 20$ . This is a rather strong result. Thus if the low  $\tan\beta$  region of  $b - \tau$  unification turns out to be the correct scenario then our analysis implies the existence of a Higgs mass below 85-90 GeV for any reasonable range of fine tuning. This scenario will be completely tested at LEP II which can allow coverage of the Higgs mass up to  $m_h \approx 95$  GeV with  $\sqrt{s} = 192$  GeV. If no Higgs is seen at LEP II then a high degree of fine tuning, i.e.  $\Phi_0 > 20$ , is indicated on the low  $\tan\beta$  end of  $b - \tau$  unification.

Further, the analysis also indicates that in order to approach the maximum allowed Higgs mass one needs to have a high degree of fine tuning. In particular from Table 2 and Fig.7 we see that going beyond 120 GeV in the Higgs mass requires a value of  $\Phi_0$  on the high side, preferably 10 and 20. The strong correlation of the Higgs mass upper limits with the value of  $\Phi_0$  has important implications for sparticle masses. Thus if the Higgs mass turns out to lie close to its allowed upper limit then a larger value of  $\Phi_0$  would be indicated. In turn a large  $\Phi_0$  would point to a heavy sparticle spectrum. At TeV33 with  $25\text{fb}^{-1}$  of integrated luminosity Higgs mass up to 120 GeV will be probed. A non-observation of the light Higgs in this mass range will imply that one needs a high degree of fine tuning which would point in the direction of heavy sparticle masses. These results are in general agreement with the analysis of Ref.[32] which arrived at much the same conclusion using a very different criterion of fine tuning. In particular the analysis of Ref.[32] also found that the non-observation of the Higgs mass below 120 GeV will imply a heavy spectrum.

## 7 Fine-tuning limits from the current experimental data

One may put limits on the fine tuning parameter using the current experimental data on sparticle searches at colliders[33, 34]. The result of this analysis is presented in Table 7. For low  $\tan\beta$  the strongest lower limits on the fine tuning parameter arise from the lower limits on the Higgs mass. In Table 7 we have used the experimental lower limits on the Higgs mass from the four detectors at LEP, i.e., the L3, OPAL, ALEPH, and DELPHI[33], to obtain lower limits on  $\Phi$  for values of  $\tan\beta$  from 2 to 20. As expected one finds that the strongest limit on  $\Phi$  arises for the smallest  $\tan\beta$ , and the constraint on  $\Phi$  falls rapidly for larger  $\tan\beta$ . Thus for  $\tan\beta$  greater than 5 the lower limit on  $\Phi$  already drops below 2 which is not a stringent fine tuning constraint. Lower limits on  $\Phi$  from the current data on the lower limits on the neutralino, the chargino, the stop, the heavy squarks, and the gluino are also analysed in Table 7. One finds that here the current lower limits on the chargino mass produce the strongest lower limit on  $\Phi$ . For  $\tan\beta$  of 2, the lower limit on  $\Phi$  from the Higgs sector is still more stringent constraint than the lower limit constraint from the chargino sector. However, for  $\tan\beta=5$  the constraint from the chargino sector becomes more stringent than the constraint from the Higgs sector. These constraints on the fine tuning will become even more stringent after LEP II completes its runs and if supersymmetric particles do not become visible.

## 8 Conclusions

In this paper we have analyzed the naturalness bounds on sparticle masses within the framework of radiative breaking of the electro-weak symmetry for minimal supergravity models and for non-minimal models with non-universal soft SUSY breaking terms. For the case of minimal supergravity it is found that for small values of  $\tan\beta$ , i.e.,  $\tan\beta \leq 5$  and a reasonable range of fine tuning, i.e.,  $\Phi \leq 20$ , the allowed values of  $m_0$  and  $m_{1/2}$  lie on the surface of an ellipsoid with the radii determined by the value of fine tuning. Specifically for the case  $\tan\beta = 2$  it is found that the upper limits on the gluino and squark masses in minimal supergravity lie within 1 TeV and the light Higgs mass lies below 90 GeV for  $\Phi_0 \leq 20$ . For  $\tan\beta \leq 5$  the upper limits of the sparticle masses all still lie within the reach of the LHC for the same range of  $\Phi_0$ . The analysis shows that the upper limits of sparticle masses are very sensitive functions of  $\tan\beta$ . As values of  $\tan\beta$  become large the loop corrections to  $\mu$  become large and the nature of the radiative breaking equation can change, i.e.,  $m_0$  and  $m_{1/2}$  may not lie on the surface of an ellipsoid. Thus it is found that there exist regions of the parameter space for large  $\tan\beta$  where the upper bounds on the sparticle masses can get very large even for reasonable values of fine tuning.

We have also analyzed the effects of non-universalities in the Higgs sector and in the third generation sector on the upper limits on the sparticle masses. It is found that non-universalities have a very significant effect on the overall size of the sparticle mass upper limits. Thus we find that the case (i)  $\delta_1 > 0$  or  $\delta_2 < 0$  and  $\delta_3 = 0 = \delta_4$  has the effect of decreasing the upper limits on the squark masses, and in contrast

the case (ii)  $\delta_1 < 0$  or  $\delta_2 > 0$  and  $\delta_3 = 0 = \delta_4$  has the effect of increasing the upper limits on the squark masses. Remarkably for  $\delta_1 = 1$ ,  $\delta_2 = -1$  and  $\delta_3 = 0 = \delta_4$  all of the sparticle masses lie below 1 TeV for  $\tan\beta \leq 5$  and  $\Phi \leq 20$  because of the non-universality effects. In this case the sparticles would not escape detection at the LHC. However, for the case  $\delta_1 = -1$ ,  $\delta_2 = 1$  and  $\delta_3 = 0 = \delta_4$  there is an opposite effect and the non-universalities raise the upper limits of the sparticle masses. Here for the same range of  $\tan\beta$ , i.e.,  $\tan\beta \leq 5$  the first and second generation squark masses can reach approximately 3 TeV for  $\Phi \leq 10$  (4-5 TeV for  $\Phi \leq 20$ ) and consequently these sparticles may escape detection even at the LHC. Similar effects occur for the non-universalities in the third generation sector. Thus non-universalities have important implications for the detection of supersymmetry at colliders.

Finally, it is found that the upper limit on the Higgs mass is a very sensitive function of  $\tan\beta$  in the region of low  $\tan\beta$  and moving the upper limit beyond 120 GeV towards its maximally allowed value will require a high degree of fine tuning. In turn large fine tuning would result in a corresponding upward movement of the upper limits of other sparticle masses. Thus a non-observation of the Higgs at the upgraded Tevatron with an integrated luminosity of  $25fb^{-1}$ , would imply a high degree of fine tuning and point to the possibility of a heavy sparticle spectrum.

#### **Acknowledgements**

Fruitful discussions with Richard Arnowitt, Howard Baer and Haim Goldberg are acknowledged. This research was supported in part by NSF grant number PHY-96020274.

## References

- [1] For a review, see P. Nath, R. Arnowitt, and A.H. Chamseddine, “Applied  $N = 1$  Supergravity” (World Scientific, Singapore, 1984); H.P. Nilles, Phys. Rep. **110**. 1 (1984).
- [2] K. Inoue et al, Prog. Theor. Phys. **68**,927(1982); L. Ibanez and G.G.Ross, Phys. Lett.**B110**,227(1982);J. Ellis, J. Hagelin, D.V. Nanopoulos, and K. Tamvakis, Phys.Lett. **125B**,275(1983); L. Alvarez-Gaume, J. Polchinski and M.B. Wise, Nucl. Phys.**B250**,495(1983).
- [3] R. Arnowitt and P. Nath, Proc. VII Swieca Summer school, ed. E. Ebohi(World Scientific, Singapore 1994).
- [4] R. Barbieri and G.F. Giudice, Nucl. Phys. **B306**,63(1988); P. Ciafaloni and A. Strumia, Nucl. Phys. **B494**, 41(1997); G. Bhattacharya and A. Romanino, Phys. Rev. **D55**, 7015(1997).
- [5] B.de. Carlos and J.A. Casas, Phys. Lett. **B309**(1993)320-328
- [6] G.W. Anderson and D.J. Castaño, Phys. Lett. **B347**,300 (1995); Phys. Rev. **D52**, 1693(1995); *ibid*,**D53**, 2403(1996).
- [7] P. Nath and R. Arnowitt, in Proc. of Les Recontres de Physique de la Vallee d’Aoste, edited by M Greco, 1992(Editions Frontiers)p.447.
- [8] V. Barger, M.S. Berger, and P. Ohmann, Phys. Lett. **B314**, 315(1993).
- [9] A.H. Chamseddine, R. Arnowitt and P. Nath, Phys. Rev. Lett. **D49**,970(1982). R. Barbieri, S. Ferrara, C. A. Savoy, Phys. Lett. **B119**, 343(1982); L. Hall, J. Lykken and S. Weinberg, Phys. Rev. **D27**, 2359(1983); P. Nath, R. Arnowitt, and A. H. Chamseddine. Nucl. Phys.**B227**, 121(1983).
- [10] G. Ross and R.G. Roberts, Nucl. Phys. **B377**, 571(1992); R. Arnowitt and P. Nath, Phys. Rev. Lett. **69**, 725(1992); M. Drees and M.M. Nojiri, Nucl. Phys. **B369**, 54(1993); S. Kelley et. al, Nucl. Phys. **B398**, 3(1993); M. Olechowski and S. Pokorski, Nucl. Phys. **B404**, 590(1993); G. Kane, C. Kolda, L. Roskowski, and J. Wells, Phys. Rev. **D49**, 6173(1994); V. Barger, M.S. Berger, and P. Ohmann, Phys. Rev. **D49**, 4908(1994); D. J. Castaño, E. Piard and P. Ramond, Phys. Rev. **D49**, 4882(1994); W. de Boer, R. Erhet and D. Kazakov, Z. Phys. **C67**, 647(1995); H. Baer, M. Baer, C. Kao, M. Nojiri, and X. Tata, Phys. Rev. **D50**, 2148(1994).
- [11] R. Arnowitt and P. Nath, Phys. Lett. **B299**, 103(1993); M. Drees and M.M. Nojiri, Phys. Rev. **D47**, 376(1993). Phys. Rev. Lett. **70**, 3696(1993); Phys. Rev. **D54**, 2374(1996); J. Lopez, D. Nanopoulos and K. Yuan, Phys. Rev. **D48**, 2766(1993); M. Drees and A. Yamada, Phys. Rev. **D53**, 1586(1996); H. Baer and M. Brhlick, Phys. Rev. **D53**, 597(1996).
- [12] V. Barger and C. Kao, hep-ph/9704403.
- [13] G. Gamberini, G. Ridolfi and F. Zwirner, Nucl. Phys. **B331**, 331(1990); R. Arnowitt and P. Nath, Phys. Rev. **D46** , 3981(1992).

- [14] L.E. Ibanez, C. Lopez and C. Munoz, Nucl. Phys. **B256** (1985) 218-252.
- [15] R. Arnowitt and P. Nath, Phys. Rev. Lett. **69**, 475(1992); P. Nath and R. Arnowitt, Phys. Lett.**B289**, 368(1992).
- [16] P. Nath and R. Arnowitt, Mod. Phys. Lett. **A2**, 331(1987); R. Arnowitt, R. Barnett, P. Nath and F. Paige, Int. Journ. Mod. Phys. **A2**, 1113(1987); R. Barbieri, F. Caravaglio, M. Frigeni, and M. Mangano, Nucl. Phys. **B367**, 28(1991); H. Baer and X. Tata, Phys. Rev. **D47**, 2739(1992); J.L. Lopez, D.V. Nanopoulos, X. Wang and A. Zichichi, Phys. Rev. **D48**, 2062(1993); H. Baer, C. Kao and X. Tata, Phys. Rev. **D48**, 5175(1993).
- [17] T. Kamon, J. Lopez, P. McIntyre and J.J. White, Phys. Rev.**D50**, 5676(1994); H. Baer, C-H. Chen, C. Kao and X. Tata, Phys. Rev. **D52**, 1565(1995); S. Mrenna, G.L. Kane, G.D. Kribbs, and T.D. Wells, Phys. Rev. **D53**, 1168(1996).
- [18] D. Amidie and R. Brock, "Report of the tev-2000 Study Group", FERMILAB-PUB-96/082.
- [19] H. Baer, C. Chen, F. Paige, and X. Tata, Phys. Rev. **D52**, 2746(1995); Phys. Rev. **D53**, 6241(1996).
- [20] The U.S. ATLAS and U.S. CMS Collaborations, LBL-38997;FERMILAB-Conf-96/432; hep-ph/9612006.
- [21] I. Hinchliffe, F.E. Paige, M.D. Shapiro, J. Soderqvist and W. Yao, Phys. Rev. **D55**, 5520(1997).
- [22] T. Tsukamoto, K. Fujii, H. Murayama, M. Yamaguchi, and Y. Okada, Phys. Rev. **D. 51**, 3153(1995).
- [23] J.L. Feng, M.E. Peskin, H. Murayama, and X. Tata, Phys. Rev. **D52**, 1418(1992).
- [24] S. Kuhlman et. al., "Physics and Technology of the NLC: Snowmass 96", hep-ex/9605011.
- [25] R. Arnowitt and P. Nath, hep-ph/9701325, Phys. Rev. **D56**, 2833(1997).
- [26] M. Carena, J.R. Espinosa, M. Quiros, and C.E.M. Wagner, Phys. Rev. **B 355**, 209(1995); M. Drees and S.P. Martin, hep-ph/9504324; H. Haber, R. Hempfling and A. Hoang, Z. Phys. **C75**, 539 (1997); H. Baer, C.-H. Chen, M. Drees, F. Paige and X. Tata, Phys. Rev. Lett. **79**, 986 (1997); J.A. Casas, J.R. Espinosa, M. Quiros and A. Riotto, Nucl. Phys. **B436** (1995) 3.
- [27] S.K. Soni and H.A. Weldon, Phys.Lett.**B126**,215(1983); V.S. Kaplunovsky and J. Louis, Phys. Lett. **B306**, 268(1993).
- [28] D. Matalliotakis and H.P. Nilles, Nucl. Phys. **B435**, 115(1995); M. Olechowski and S. Pokorski, Phys.Lett. **B344**, 201(1995).
- [29] V. Berezhinsky, A. Bottino, J. Ellis, N. Forrengo, G. Mignola, and S. Scopel, Astropart. Phys. 5:1-26(1996); ibid, 5:333(1996).
- [30] P. Nath and R. Arnowitt, hep-ph/9701301, Phys. Rev **D56**, 2820(1997).

- [31] Effects of non-universalities on the upper limits of sparticle masses in the context of the fine tuning criterion of Ref.[4] is discussed in S. Dimopoulos and G. Giudice, Phys. Lett.**B357**, 573(1995).
- [32] G.W. Anderson, D.J.Castaño and A. Riotto, Phys. Rev. **D55**, 2950(1997).
- [33] Joachim Mnich, *LEP Physics - An Overview*, plenary talk at The Sixth International Symposium on PARTICLES, STRINGS and COSMOLOGY, PASCOS-98, Boston, Massachusetts, March 22-29, 1998; Joachim Mnich, *Results of the L3 Experiment at 183 GeV*, presentation at CERN LEPC, 31 March 1998; John Carr, *ALEPH Status Report*, presentation at CERN LEPC, 31 March 1998; Klaus Moenig, *DELPHI Results at 183 GeV*, presentation at CERN LEPC, 31 March 1998; Mark Thomson, *OPAL Physics Highlights at  $\sqrt{s}=183$  GeV*, presentation at CERN LEPC, 31 March 1998.
- [34] [http://wwwd0.fnal.gov/public/new\\_public.html](http://wwwd0.fnal.gov/public/new_public.html).



Scale dependence of $C_1 - C_4$					
$\tan\beta$	$Q(GeV)$	$C_1$	$C_2$	$C_3$	$C_4$
2	91.2	0.7571	0.0711	4.284	0.3119
	2000	0.6874	0.0879	2.851	0.3073
	4000	0.6702	0.0918	2.607	0.3055
	6000	0.6598	0.0941	2.474	0.3043
	8000	0.6523	0.0957	2.384	0.3034
	10000	0.6464	0.0970	2.316	0.3026
5	91.2	0.14212	0.1024	2.871	0.4491
	500	0.09016	0.1099	2.200	0.4245
	1000	0.06843	0.1126	1.973	0.4138
	1500	0.05558	0.1142	1.851	0.4074
	2000	0.04639	0.1152	1.768	0.4028
	2500	0.03924	0.1160	1.706	0.3992
	3000	0.03336	0.1166	1.657	0.3962
	3500	0.02838	0.1172	1.617	0.3937
	4000	0.02406	0.1176	1.583	0.3914
	4500	0.02023	0.1180	1.553	0.3895
	5000	0.01680	0.1184	1.527	0.3877
10	91.2	0.0756	0.1040	2.710	0.4561
	250	0.0446	0.1081	2.305	0.4397
	500	0.0230	0.1108	2.062	0.4280
	750	0.0102	0.1122	1.931	0.4211
	1000	0.0011	0.1132	1.843	0.4160
	1250	-0.0060	0.1140	1.778	0.4121
	1500	-0.0118	0.1146	1.726	0.4089
	1750	-0.0167	0.1151	1.683	0.4061
	2000	-0.0210	0.1155	1.646	0.4037
	2500	-0.0281	0.1162	1.587	0.3997
	3000	-0.0341	0.1167	1.540	0.3964
20	250	0.02850	0.1084	2.269	0.4406
	500	0.00685	0.1109	2.029	0.4286
	750	-0.00592	0.1123	1.899	0.4214
	1000	-0.01504	0.1133	1.812	0.4162
	1250	-0.02213	0.1140	1.747	0.4122
	1500	-0.02795	0.1146	1.695	0.4089
	1750	-0.03288	0.1150	1.653	0.4061
	2000	-0.03716	0.1154	1.617	0.4036
	2500	-0.04433	0.1161	1.558	0.3995
	3000	-0.05020	0.1166	1.511	0.3961

Table 1: The scale dependence of  $C_1(Q) - C_4(Q)$  for minimal supergravity when  $m_t = 175 \text{ GeV}$  for  $\tan\beta = 2, 5, 10$  and  $20$ .

Minimal Supergravity $\mu < 0$													
$\tan \beta$	$\Phi$	H	$\tilde{u}_l$	$\tilde{e}_l$	$\tilde{e}_r$	$\tilde{t}_1$	$\tilde{t}_2$	$\tilde{g}$	h	$\tilde{\chi}_1^\pm$	$\tilde{\chi}_2^\pm$	$\tilde{\chi}_1^0$	$m_0$
2	5	326	290	212	207	264	325	316	69	102	224	48	204
	10	479	419	320	315	353	429	459	78	139	303	67	315
	20	687	598	463	459	483	579	649	86	190	419	94	459
5	2.5	318	352	292	285	265	352	295	97	77	180	42	282
	5	594	589	560	556	365	507	425	103	114	232	60	556
	10	930	906	888	884	510	744	610	109	167	309	86	886
	20	1417	1381	1368	1365	742	1113	873	116	243	423	123	1368
10	2.5	416	464	403	393	323	431	316	106	73	184	42	395
	5	3702	4089	3914	3887	2311	3311	1272	136	190	382	158	3920
	10	5963	6714	6365	6318	3855	5428	2776	144	283	797	273	6370
	20	8875	10536	9622	9527	6170	8616	4945	150	404	1409	400	9596
20	2.5	1889	2136	2044	2003	1202	1697	566	128	104	214	69	2080
	5	3581	4198	3906	3827	2480	3383	1764	138	194	515	178	3980
	10	5540	6585	6114	5978	3893	5270	3124	145	282	895	274	6210
	20	8007	10092	8954	8734	6078	8167	5322	151	403	1516	399	9060

Table 2: The upper bound on sparticle masses for minimal supergravity when  $m_t = 175 \text{ GeV}$  and  $\mu < 0$  for different values of  $\tan\beta$  and fine tuning measure  $\Phi_0$ . All the masses are in GeV.

$\tan \beta$	$\delta_1$	$\delta_2$	$C'_1$
2	-1.0	1.0	-0.341
	-0.75	0.75	-0.067
	-0.5	0.5	0.208
	-0.25	0.25	0.483
	0.0	0.0	0.757
	0.25	-0.25	1.032
	0.5	-0.5	1.306
	0.75	-0.75	1.581
	1.0	-1.0	1.855
5	-1.0	1.0	-0.572
	-0.75	0.75	-0.393
	-0.5	0.5	-0.215
	-0.25	0.25	-0.036
	0.0	0.0	0.142
	0.25	-0.25	0.321
	0.5	-0.50	0.499
	0.75	-0.75	0.677
	1.0	-1.0	0.856
10	-1.0	1.0	-0.597
	-0.75	0.75	-0.429
	-0.5	0.5	-0.261
	-0.25	0.25	-0.092
	0.0	0.0	0.076
	0.25	-0.25	0.244
	0.5	-0.5	0.412
	0.75	-0.75	0.580
	1.0	-1.0	0.748
20	-1.0	1.0	-0.603
	-0.75	0.75	-0.437
	-0.5	0.5	-0.272
	-0.25	0.25	-0.106
	0.0	0.0	0.060
	0.25	-0.25	0.225
	0.5	-0.5	0.391
	0.75	-0.75	0.556
	1.0	-1.0	0.722

Table 3:  $C'_1(M_Z)$  for different values of  $\delta_1$  and  $\delta_2$  when  $m_t = 175 \text{ GeV}$  for  $\tan\beta = 2, 5, 10$  and 20.

Non-universal case: $(\delta_1, \delta_2, \delta_3, \delta_4) = (1, -1, 0, 0)$ , $\mu < 0$													
$\tan \beta$	$\Phi$	H	$\tilde{u}_l$	$\tilde{e}_l$	$\tilde{e}_r$	$t_1$	$t_2$	$\tilde{g}$	h	$\tilde{\chi}_1^\pm$	$\tilde{\chi}_2^\pm$	$\tilde{\chi}_1^0$	$m_0$
2	5	313	291	148	140	267	328	319	70	104	225	49	134
	10	457	419	220	207	354	430	459	79	140	304	68	205
	20	655	601	317	296	488	585	656	87	193	420	95	299
5	2.5	213	274	133	121	243	336	301	95	79	181	44	109
	5	356	391	221	228	324	430	429	103	115	233	62	204
	10	535	569	334	312	462	580	620	110	170	310	89	315
	20	775	841	485	451	677	820	915	116	254	425	130	462
10	2.5	203	285	129	103	246	349	316	104	74	185	43	93
	5	371	406	234	216	333	447	446	110	112	237	62	215
	10	559	583	357	332	471	598	637	116	169	314	90	338
	20	810	843	520	483	680	828	920	122	251	427	130	496
20	2.5	216	286	125	69	242	350	315	105	69	186	40	75
	5	383	409	236	203	330	451	448	111	109	237	60	216
	10	577	590	357	323	472	604	646	117	167	315	89	343
	20	843	854	519	479	687	835	932	122	252	428	130	508

Table 4: The upper bounds on sparticle masses for the case of non-universalities in the Higgs sector when  $(\delta_1, \delta_2) = (1, -1)$ ,  $\delta_3 = 0 = \delta_4$ ,  $m_t = 175 \text{ GeV}$ , and  $\mu < 0$  for different values of  $\tan \beta$  and  $\Phi$ . All the masses are in GeV.

$(\delta_1, \delta_2, \delta_3, \delta_4) = (-1, 1, 0, 0)$					
$\tan \beta$	$Q(GeV)$	$C'_1$	$C_2$	$C_3$	$C_4$
2	91.2	-0.341	0.071	4.284	0.312
	250	-0.363	0.0765	3.742	0.3110
	500	-0.378	0.0802	3.415	0.3101
	750	-0.387	0.0825	3.239	0.3094
	1000	-0.394	0.0841	3.119	0.3089
	1250	-0.399	0.0853	3.030	0.3084
	1500	-0.404	0.0863	2.959	0.3080
	1750	-0.408	0.0872	2.901	0.3077
	2000	-0.411	0.0879	2.851	0.3073
5	91.2	-0.572	0.1024	2.871	0.4491
	250	-0.602	0.1069	2.452	0.4348
	500	-0.624	0.1099	2.200	0.4245
	750	-0.636	0.1115	2.064	0.4183
	1000	-0.645	0.1126	1.973	0.4138
	1250	-0.652	0.1135	1.905	0.4103
	1500	-0.658	0.1142	1.851	0.4074
	1750	-0.663	0.1147	1.806	0.4049
	2000	-0.667	0.1152	1.768	0.4028
10	91.2	-0.597	0.1040	2.710	0.4561
	250	-0.628	0.1081	2.305	0.4397
	500	-0.649	0.1108	2.062	0.4280
	750	-0.662	0.1122	1.931	0.4211
	1000	-0.671	0.1132	1.843	0.4160
	1250	-0.678	0.1140	1.778	0.4121
	1500	-0.684	0.1146	1.726	0.4089
	1750	-0.689	0.1151	1.683	0.4061
	2000	-0.693	0.1155	1.646	0.4037
20	91.2	-0.603	0.1043	2.671	0.4575
	250	-0.634	0.1084	2.269	0.4406
	500	-0.655	0.1109	2.029	0.4286
	750	-0.668	0.1123	1.899	0.4214
	1000	-0.677	0.1133	1.812	0.4162
	1250	-0.684	0.1140	1.747	0.4122
	1500	-0.690	0.1146	1.695	0.4089
	1750	-0.695	0.1150	1.653	0.4061
	2000	-0.699	0.1154	1.617	0.4036

Table 5: The scale dependence of  $C'_1(Q), C_2(Q) - C_4(Q)$  for  $(\delta_1, \delta_2, \delta_3, \delta_4) = (-1, 1, 0, 0)$  for  $m_t = 175 \text{ GeV}$  and  $\tan \beta = 2, 5, 10$  and 20.

$(\delta_1, \delta_2, \delta_3, \delta_4) = (0, 0, 1, 0), \quad \mu < 0$													
$\tan \beta$	$\Phi$	H	$\tilde{u}_l$	$\tilde{e}_l$	$\tilde{e}_r$	$\tilde{t}_1$	$\tilde{t}_2$	$\tilde{g}$	h	$\tilde{\chi}_1^\pm$	$\tilde{\chi}_2^\pm$	$\tilde{\chi}_1^0$	$m_0$
2	5	290	292	162	140	266	326	319	70	104	225	49	147
	10	418	419	242	211	351	429	456	79	139	304	68	226
	20	597	601	349	306	486	583	656	87	193	420	95	331
5	2.5	198	275	151	125	244	337	301	95	79	181	44	126
	5	325	391	258	223	325	430	429	103	115	233	62	239
	10	485	559	389	340	453	573	611	110	168	310	87	368
	20	702	807	571	501	652	791	880	116	245	424	125	546
10	2.5	194	291	144	110	247	349	316	104	74	185	43	110
	5	342	422	279	239	333	445	446	110	112	237	62	259
	10	514	606	428	371	471	599	637	116	169	314	90	407
	20	747	870	629	549	680	828	920	122	251	427	130	604
20	2.5	213	293	134	77	245	352	316	106	70	187	41	88
	5	360	431	281	229	331	452	449	112	110	238	61	261
	10	541	621	433	364	473	605	646	118	168	316	90	416
	20	804	894	638	543	688	836	932	123	252	429	131	620

Table 6: The upper bound on sparticle masses for non-universalities in the third generation when  $(\delta_3, \delta_4) = (1, 0)$ ,  $m_t = 175 GeV$ , and  $\mu < 0$  for different values of  $\tan \beta$  and  $\Phi$ . All the masses are in GeV.

$\sqrt{s} = 183$ GeV LEP 95% C.L.lower bound on $m_h$		
$\tan \beta$	mass lower bdd (GeV)	$\Phi(\mu < 0)$
2	86 (L3)	20
	74 (OPAL scan B)	8
	88 (ALEPH)	23
	84 (DELPHI)	18
5	72 (L3)	$< 2$
	71 (OPAL scan B)	
	73 (ALEPH)	
	76 (DELPHI)	
10	72 (L3)	$< 2$
	70 (OPAL scan B)	
	76 (ALEPH)	
	75 (DELPHI)	
20	71 (L3)	$< 2$
	70 (OPAL scan B)	
	76 (ALEPH)	
	76 (DELPHI)	
$\sqrt{s} = 183$ GeV LEP 95% C.L. lower bounds on various sprticles masses		
Particle	mass lower bdd (GeV)	$\Phi(\mu < 0)$
$\chi^0$	24 independent of $m_0$ (DELPHI)	$< 1.5$ for $\tan \beta \geq 2$ $< 1.5$
	14 any $m_0$ (ALEPH)	
	27 for $\tan \beta = 2$ (L3)	
$\chi^\pm$	51 (ALEPH)	$< 1.5$ for $\tan \beta \geq 2$
$\tilde{t}$	$\tilde{t} \rightarrow c\chi$ $m_{\tilde{t}} > 74$ (ALEPH) $\tilde{t} \rightarrow b\nu\chi$ $m_{\tilde{t}} > 82$ (ALEPH)	$< 1.5$ for $\tan \beta \geq 2$
95% C.L. lower bounds on various sprticles masses from ref[34]		
Particle	mass lower bdd (GeV)	$\Phi(\mu < 0)$
$\chi^\pm$	$m_{\chi^\pm} > 45, .66$ pb	$< 1.5$
	$m_{\chi^\pm} > 124, .01$ pb	$\Phi > 8, \tan \beta = 2$ $\Phi > 5.8, \tan \beta = 5$
$\tilde{q} \tilde{g}$	$m_{\tilde{g}} > 230$ , heavy squarks	$\Phi > 2.7, \tan \beta = 2$
	$m_{\tilde{q}, \tilde{g}} > 260, m_{\tilde{q}} = m_{\tilde{g}}$	$\Phi > 4.0, \tan \beta = 2$ $\Phi < 1.8, \tan \beta \geq 5$
	$m_{\tilde{q}} > 219$ , heavy gluinos	$\Phi > 2.8, \tan \beta = 2$ $\Phi < 1.8, \tan \beta \geq 5$

Table 7: Current experimental lower bounds on masses of the lightest Higgs and various sparticles from LEP and the Tevatron. Corresponding fine-tunings ( $\mu < 0$ ) are also shown.

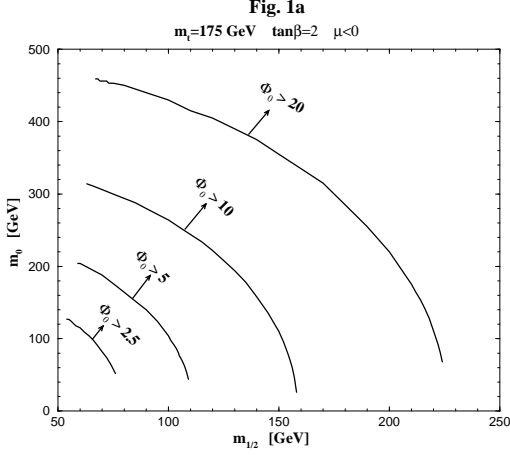


Fig.1a. Contour plot of the upper limit in the  $m_0 - m_{\frac{1}{2}}$  plane for different values of  $\Phi_0$  when  $m_t = 175 \text{ GeV}$ ,  $\tan\beta = 2$  and  $\mu < 0$ . The allowed region lies below the curves.

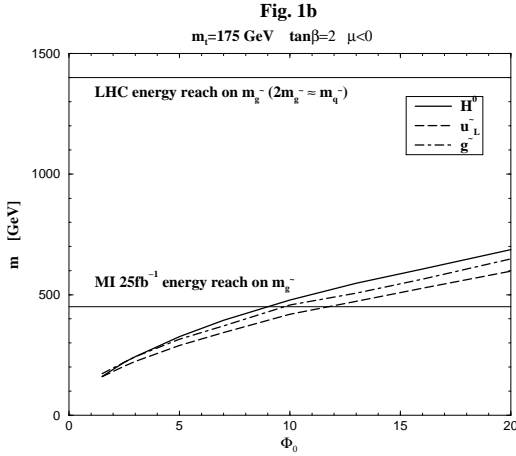


Fig.1b. Upper bounds on mass of the heavy Higgs  $H^0$ , of the gluino and of the squark  $\tilde{u}_L$  (for the first two generations) for the same parameters as in Fig.1a.

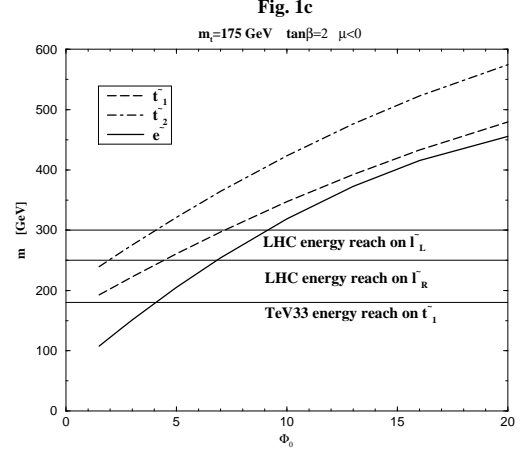


Fig.1c. Upper bounds on mass of the  $\tilde{e}_L$ , of the light stop  $\tilde{t}_1$ , and of the heavy stop  $\tilde{t}_2$  for the same parameters as in Fig.1a.

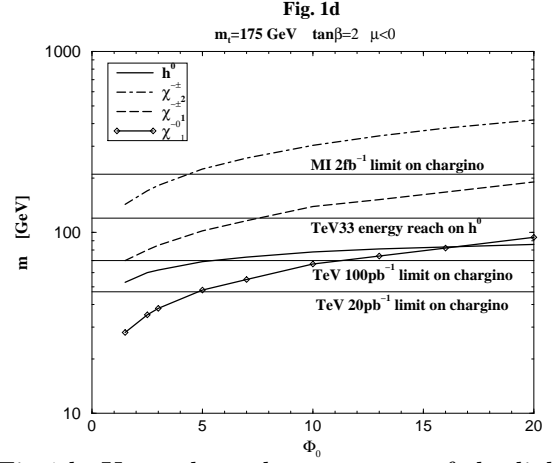


Fig.1d. Upper bounds on masses of the light Higgs  $h^0$ , of the light chargino  $\tilde{\chi}_1^\pm$ , of the heavy chargino  $\tilde{\chi}_2^\pm$ , and of the neutralino  $\tilde{\chi}_1^0$  for the same parameters as in Fig.1a.



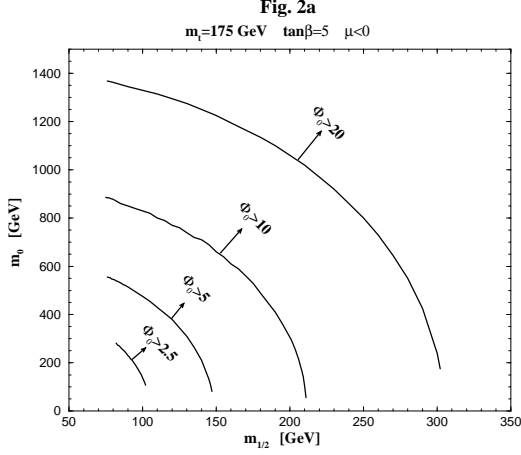


Fig.2a. Contour plot of the upper limit in the  $m_0 - m_{\frac{1}{2}}$  plane for different values of  $\Phi_0$  when  $m_t = 175 \text{ GeV}$ ,  $\tan\beta = 5$  and  $\mu < 0$ . The allowed region lies below the curves.

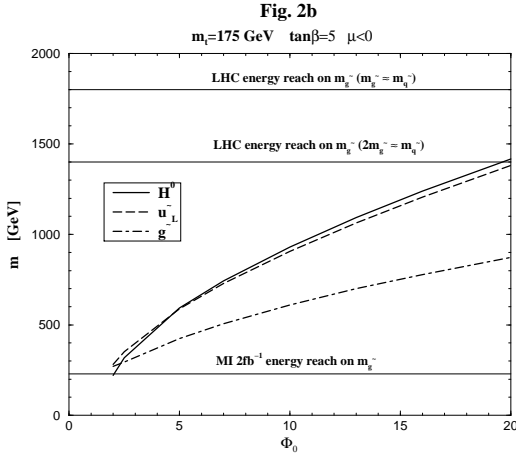


Fig.2b. Upper bounds on mass of the heavy Higgs  $H^0$ , of the gluino and of the squark  $\tilde{u}_L$  (for the first two generations) for the same parameters as in Fig.2a.

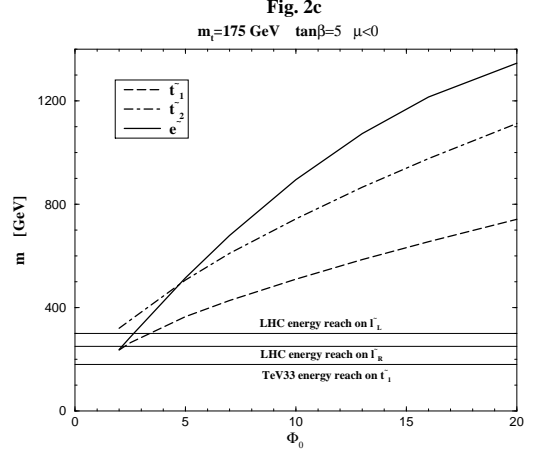


Fig.2c. Upper bounds on mass of the  $\tilde{e}_L$ , of the light stop  $\tilde{t}_1$ , and of the heavy stop  $\tilde{t}_2$  for the same parameters as in Fig.2a.

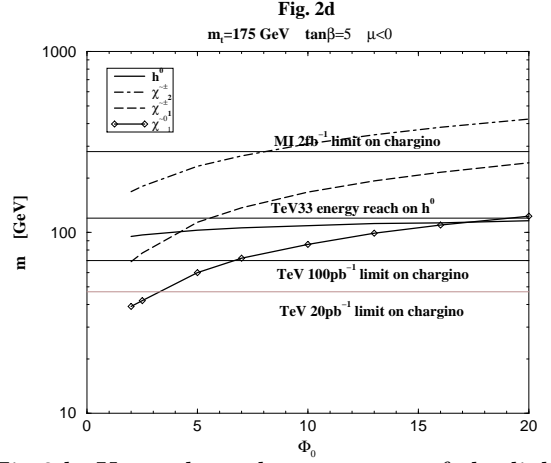


Fig.2d. Upper bounds on masses of the light Higgs  $h^0$ , of the light chargino  $\tilde{\chi}_1^\pm$ , of the heavy chargino  $\tilde{\chi}_2^\pm$ , and of the neutralino  $\tilde{\chi}_1^0$  for the same parameters as in Fig.2a.

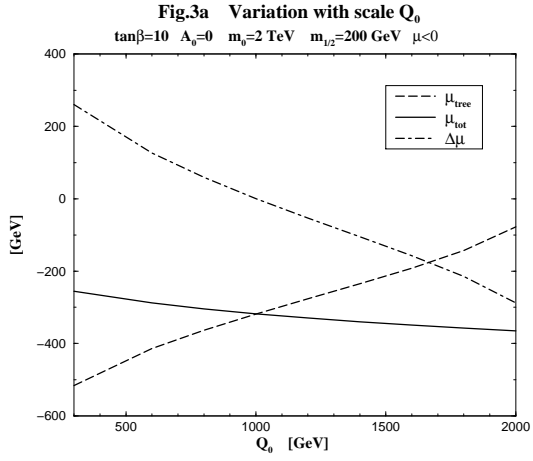


Fig.3a. Variation of  $\mu$  with the scale  $Q_0$  where the minimization of the potential is carried out for the case when  $\tan\beta = 10$ ,  $A_0 = 0$ ,  $m_0 = 2000\text{GeV}$ ,  $m_{1/2} = 200$  GeV and  $\mu < 0$ .

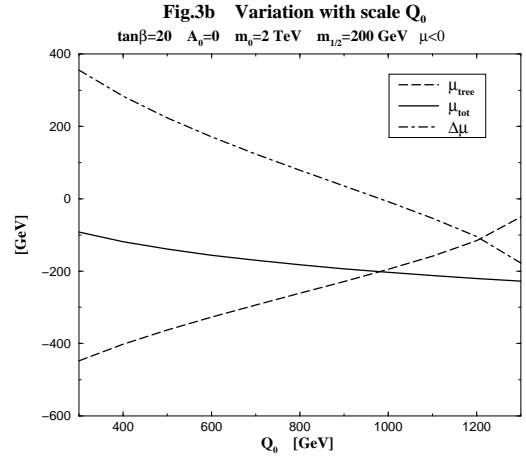


Fig.3b. Variation of  $\mu$  with the scale  $Q_0$  where the minimization of the potential is carried out for the case when  $\tan\beta = 20$ , with the other parameters the same as in Fig.3a.

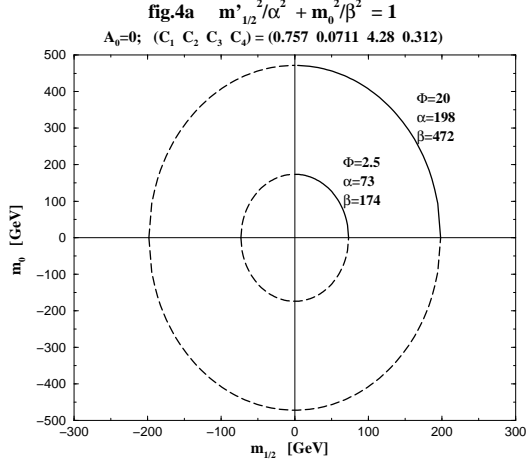


Fig.4a. Diagrammatic illustration of the ellipse represented by Eq.(12), where the values of  $C_1 - C_4$  are for  $\tan\beta=2$  and  $Q = M_Z$  from Table 1. The relevant parts of the ellipses are in solid line.

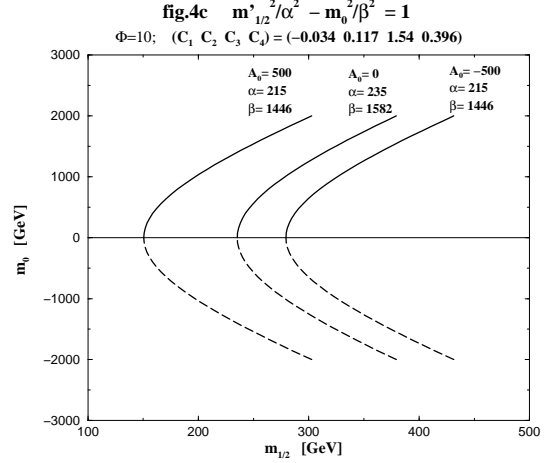


Fig.4c. Diagrammatic illustration of the hyperbola represented by Eq.(14) and Eq.(28), where the values of  $C_1 - C_4$  are for  $\tan\beta=10$  and  $Q=3000$  GeV from Table 1. The relevant parts of the hyperbolae are in solid line.

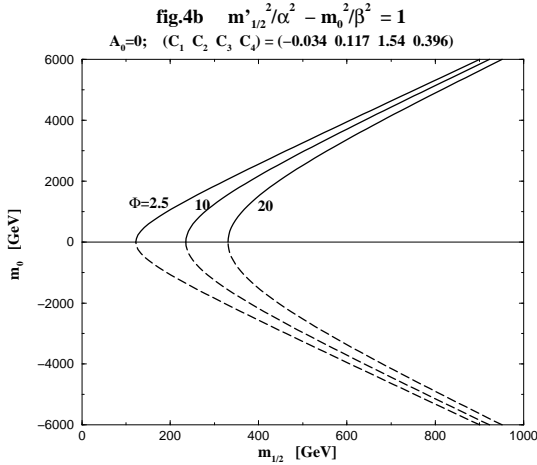


Fig.4b. Diagrammatic illustration of the hyperbola represented by Eq.(14) and Eq.(28), where the values of  $C_1 - C_4$  are for  $\tan\beta=10$  and  $Q=3000$  GeV from Table 1. The relevant parts of the hyperbolae are in solid line.

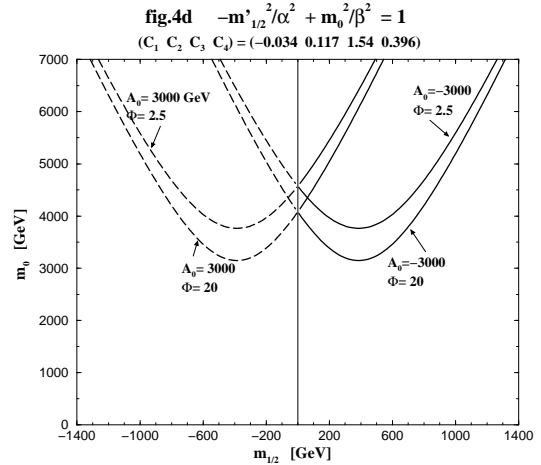


Fig.4d. Diagrammatic illustration of the hyperbola represented by Eq.(19) and Eq.(30), where the values of  $C_1 - C_4$  are for  $\tan\beta=10$  and  $Q=3000$  GeV from Table 1. The relevant parts of the hyperbolae are in solid line.

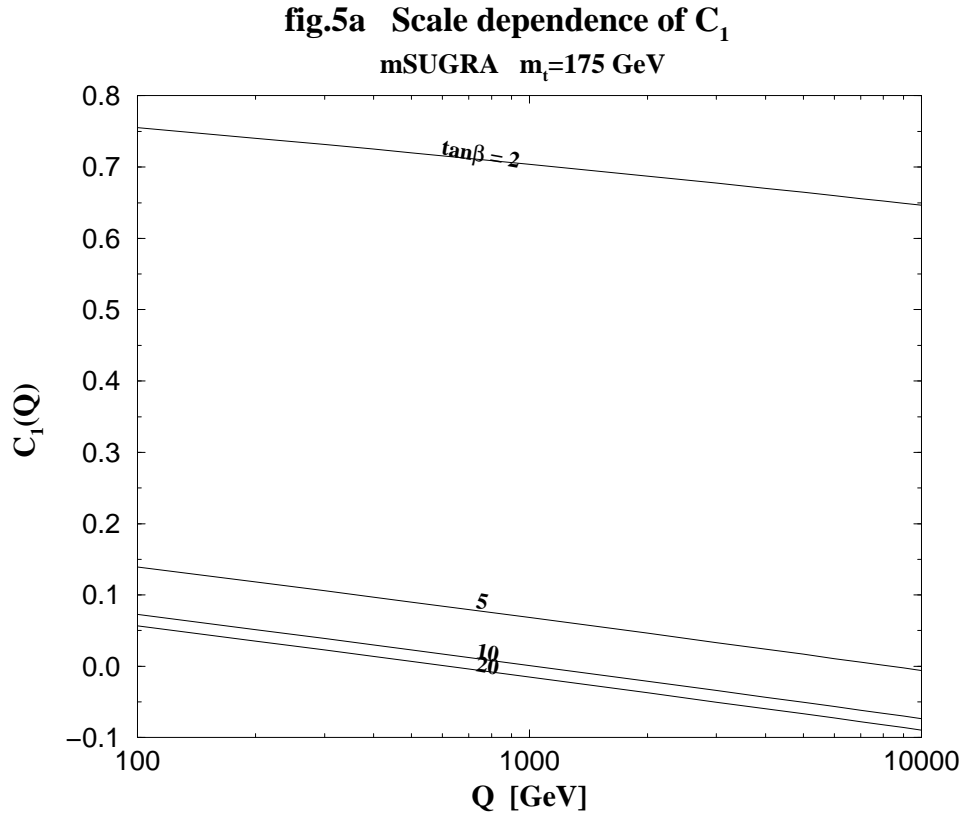


Fig.5a. The scale dependence of  $C_1(Q)$  for minimal supergravity when  $m_t = 175$  GeV for  $\tan\beta = 2, 5, 10$  and  $20$ .

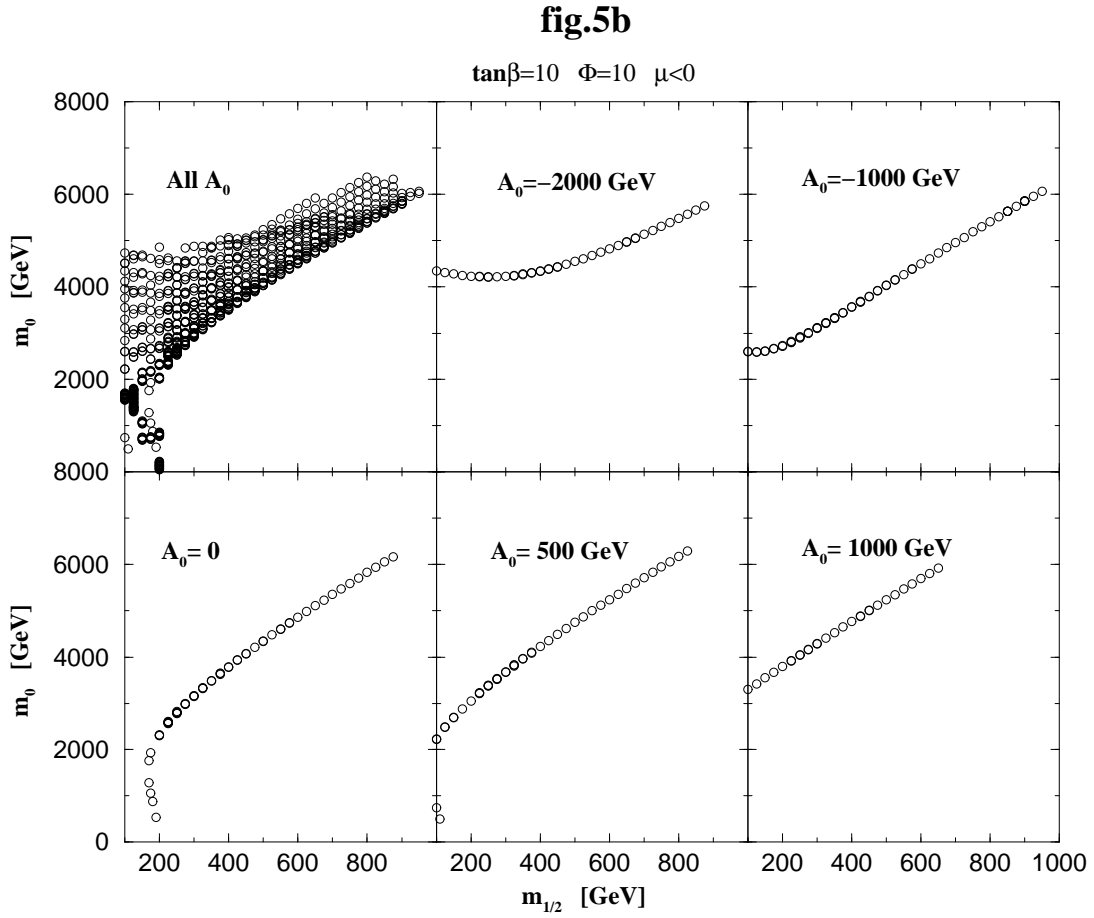


Fig.5b. Allowed region in the  $m_0 - m_{1/2}$  plane in the minimal supergravity case for  $m_t = 175$  GeV,  $\tan\beta=10$ ,  $\Phi_0 = 10$  and negative  $\mu$ .

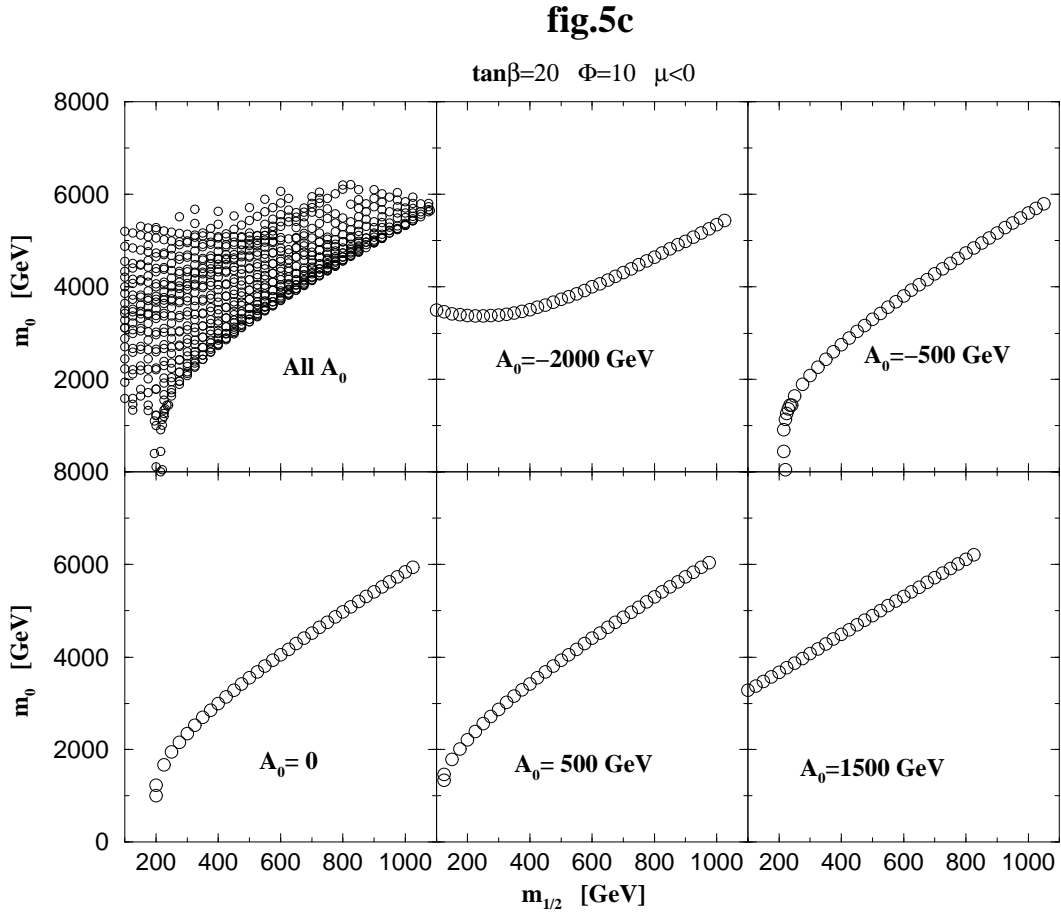


Fig.5c. Allowed region in the  $m_0 - m_{1/2}$  plane in the minimal supergravity case for  $m_t = 175$  GeV,  $\tan\beta=20$ ,  $\Phi_0 = 10$  and negative  $\mu$ .

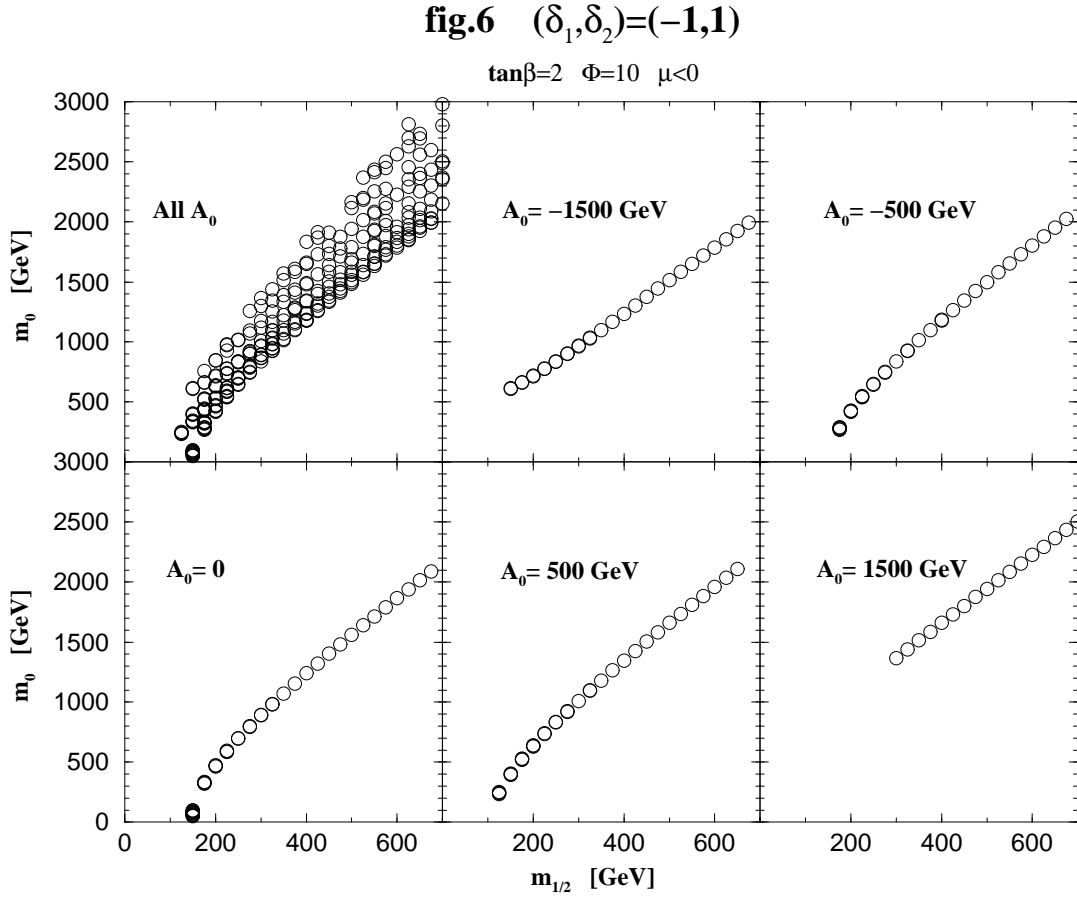


Fig.6. Allowed region in the  $m_0 - m_{1/2}$  plane under the non-universal boundary condition of  $(\delta_1, \delta_2) = (-1, 1)$  for  $m_t = 175$  GeV,  $\tan\beta=2$ ,  $\Phi=10$  and negative  $\mu$ .

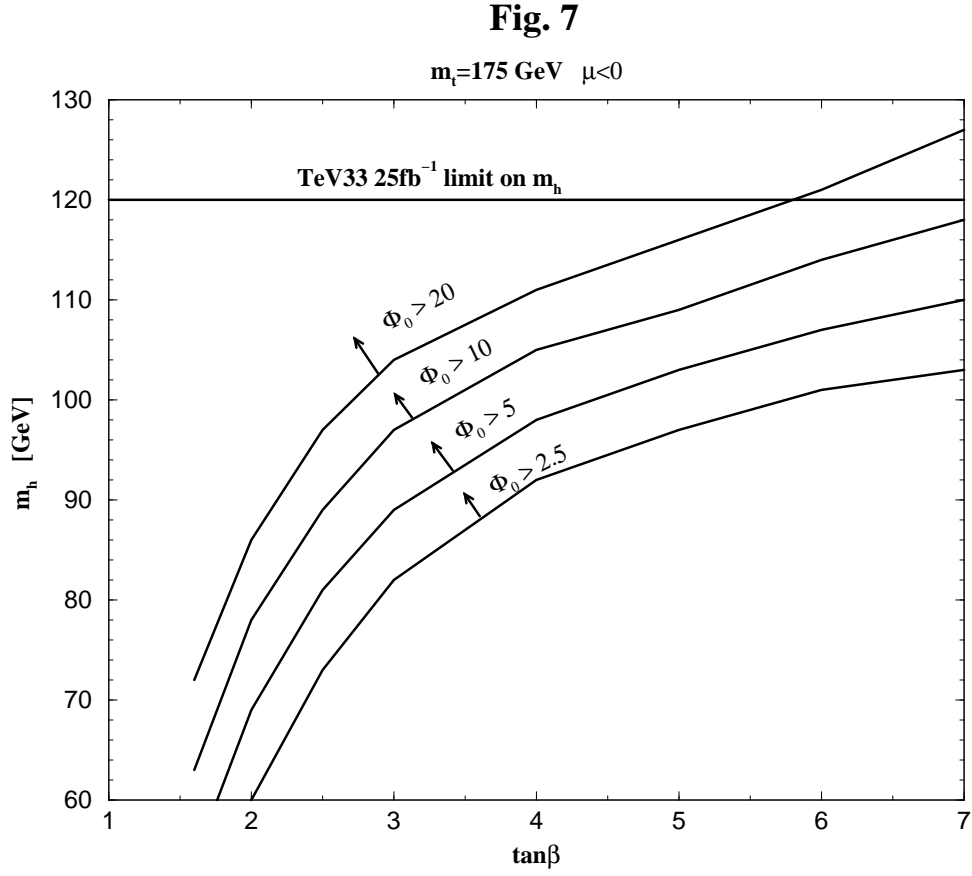


Fig.7. Upper bounds on the light Higgs  $h^0$  mass for different values of  $\Phi_0$  as a function of  $\tan\beta$  when  $m_t = 175 \text{ GeV}$  and  $\mu < 0$ .